



## DIFFUSION IN THE NICKEL-RHENIUM SYSTEM

C.M. Neubauer\*, D. Mari\*\* and D.C. Dunand

Department of Materials Science and Engineering, Massachusetts Institute of Technology, Cambridge, MA 02139, USA

\*currently at the Department of Materials Science and Engineering, Northwestern University, Evanston, IL 60201, USA

\*\*currently at Amysa, 10 Route de Lausanne, 1400 Yverdon, Switzerland.

(Received December 7, 1993)

(Revised March 21, 1994)

Most nickel-based metal matrix composites (MMC) studied to date were reinforced with ductile refractory metal fibers, mostly tungsten or tungsten-alloys (1-2). However, nickel embrittles and weakens cold-drawn tungsten fibers by (i) forming intermetallic phases at the fiber-matrix interface (3-4) and (ii) inducing recrystallization of tungsten at temperatures as low as 950°C by rapid grain-boundary diffusion (1-2, 5-6). To prevent these problems, ceramic coatings with low solubility, reactivity, and diffusion coefficients for both tungsten and nickel can be applied at the interface (2). However, ceramic coatings are brittle, and typically exhibit a large mismatch of coefficient of thermal expansion with nickel; therefore, these coatings tend to crack when the composite is subjected to thermal cycling (2, 7).

To prevent cracking of the diffusion barrier, ductile, metallic coatings can be used. Rhenium is an attractive candidate for tungsten fibers in a nickel matrix, since it exhibits high-temperature strength significantly higher than tungsten, while retaining excellent ductility at all temperatures, even after recrystallization (8, 9). Also, its coefficient of thermal expansion is between those of tungsten and nickel (10). Diffusion in the Re-W system at the potential use temperatures of Ni-based MMC (1200-1500 K) is negligible due to the very high melting points of both tungsten and rhenium (3695 K and 3459 K, respectively). Furthermore, rhenium additions have been found to improve the mechanical properties of both tungsten and nickel (11). Finally, the Ni-Re phase diagram shows a simple peritectic system with no intermetallic present (Fig. 1). However, one potential drawback is the relatively high solubility of each metal in the other.

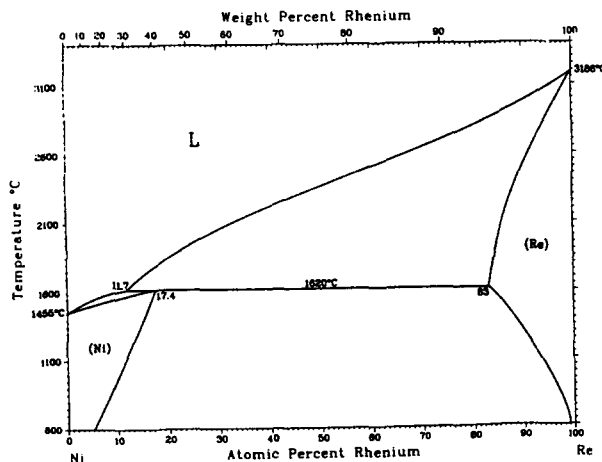


FIG. 1 - Ni-Re phase diagram (14).

In what follows, we present an experimental investigation of diffusion phenomena in the Ni-Re system. The parameters controlling diffusion (activation energy and frequency factor) of each metal into the other are determined in order to predict long-term diffusion behavior at elevated temperatures and to assess the suitability of rhenium diffusion coatings for tungsten fibers in nickel-based matrices.

### **Experimental Procedures**

A layer of 99.999% pure nickel approximately 60  $\mu\text{m}$  thick was deposited onto a 100  $\mu\text{m}$  thick rhenium foil (99.99% pure, obtained from Aesar, MA) with a Sloan E-beam evaporator under a vacuum of  $6 \cdot 10^{-4}$  Pa at a working distance of 51 mm. Three depositions occurred for a total time of 545 seconds, with the vacuum being broken between each deposition. The Ni-Re specimen was then cut into 5 mm x 5 mm diffusion couples, which were encapsulated in evacuated quartz tubes containing a tantalum getter and annealed at temperatures between 990  $^{\circ}\text{C}$  and 1110  $^{\circ}\text{C}$  for times between 50 h and 228 h (Table 1). The heating rate was 720 K/h and rapid cooling at the end of the anneal was reached by removing the capsules from the furnace and allowing them to air-cool.

Following annealing, each diffusion couple was mounted in bakelite with the Ni-Re interface perpendicular to the plane of polish, ground on silicon carbide, and polished using alumina and diamond pastes. The metallographic procedures removed at least 100  $\mu\text{m}$  from the sample, ensuring that the bulk material was observed. Polished samples were examined by optical microscopy and scanning electron microscopy in back-scatter mode. Carbon-coated polished samples were further analyzed by electron microprobe (Jeol Superprobe 733) with a 1  $\mu\text{m}$  beam width, calibrated with pure nickel and rhenium samples. Three composition profiles perpendicular to the Ni-Re interface were measured for each sample with a step length of 2  $\mu\text{m}$ .

### **Results and Discussion**

Figure 2a shows that for unannealed Sample 1 the Ni-Re interface is planar, pore-free, and well bonded. The interface of Sample 5, annealed for 228 hours at 1323 K, is slightly more wavy, the maximum amplitude being about 3  $\mu\text{m}$  (Fig. 2b). Neither Kirkendall porosity nor intermetallic phases are observed. Figure 2b is representative of the structure of all the other annealed samples.

Figures 3a and 3b show the average diffusion profiles as a function of annealing time and temperature, respectively. While the diffusion profile of rhenium in nickel has the expected shape and curvature for the simple case of the error function solution, the diffusion profiles of nickel in rhenium exhibit a shallow con-

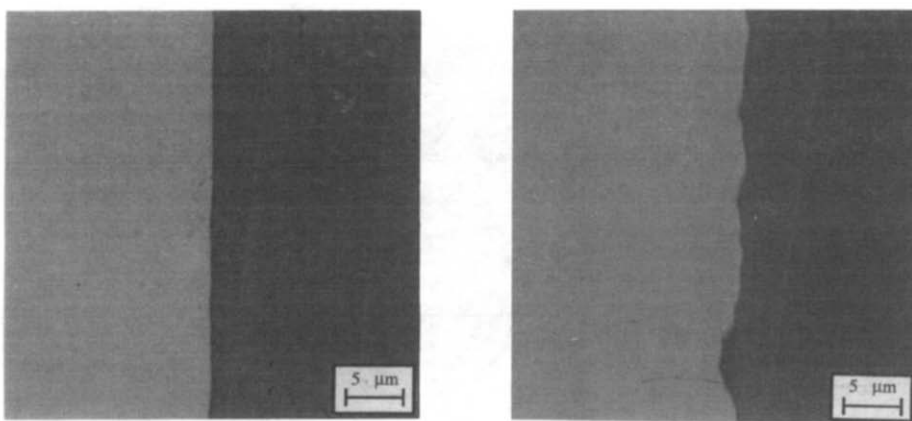


**FIG. 2** - Back-scattered scanning electron micrograph of Sample 1 (a) and Sample 5 (b). Nickel is dark, rhenium is bright.

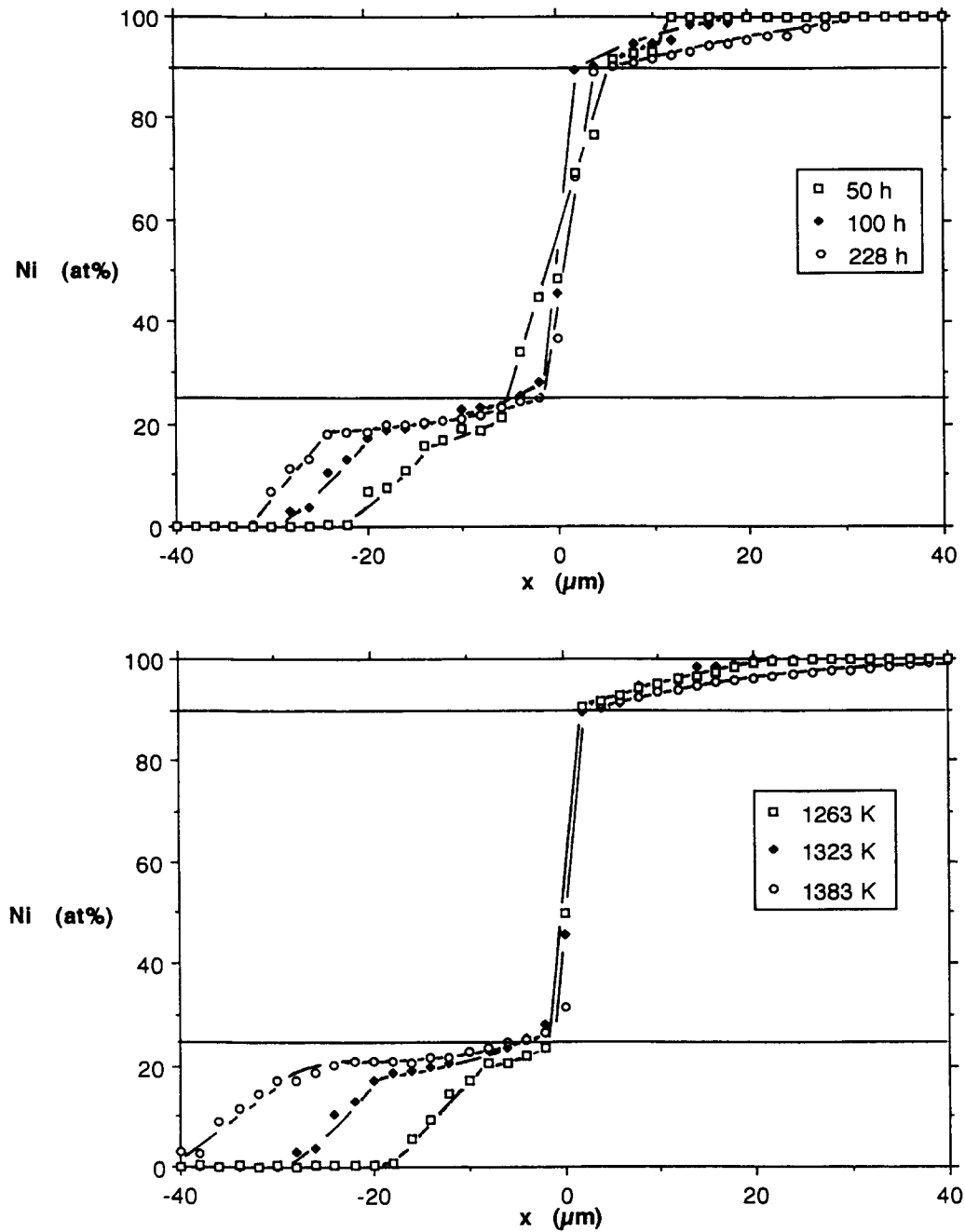


FIG. 3 - Concentration profiles of Ni-Re diffusion couples.

(a) annealed at 1323 K between 50 h and 228 h and (b) annealed between 1263 K and 1383 K for 100 h.

TABLE 1 - Annealing Temperatures, Annealing Times and Diffusion Depths.

Sample	Annealing Temperature (K)	Annealing Time (h)	Diffusion Depth Ni in Re * ( $\mu\text{m}$ )	Diffusion Depth Re in Ni * ( $\mu\text{m}$ )
1	unannealed	—	4	0
2	1263	100	14	16
3	1323	50	14	6
4	1323	100	24	16
5	1323	228	28	24
6	1383	100	36	36

\* error:  $\pm 2 \mu\text{m}$ 

centration gradient at high nickel concentration, followed by a steeper gradient at lower nickel concentrations. The shape of the diffusion profile indicates that the chemical diffusion coefficient is concentration-dependent in the range 0-25 at% Ni (12). The other possible explanation for the shape of the profile - the presence of an intermetallic phase at a concentration of about 20 at% Ni - is supported neither by the metallographic examination (Fig. 2b) nor by other investigations of the Ni-Re phase system reviewed in Ref. (13). Furthermore, the gradually declining concentration profile observed between 20 at% Ni and 0 at% Ni is not coherent with the sharp interface expected between an intermetallic phase and a rhenium-rich solid solution.

Figures 3a and 3b show a rhenium solubility in nickel of about 10 at% Re, and a nickel solubility in rhenium of about 25 at% Ni at the temperatures investigated. While the former value is in agreement with the Ni-Re phase diagram (14) (Fig. 1), the latter value is much higher than the solubility of 3-7 at% Ni reported in that phase diagram or the solubility of 8-10 at% Ni in the diagram published by Nash and Nash (13). The latter authors reviewed the work of other researchers who found widely different, and mutually exclusive, values for the solubility of nickel into rhenium: 18 at% Ni and 58 at% Ni at 1893 K, 45 at% Ni and 52 at% Ni at 1473 K, and 14 at% Ni at 1073 K.

Table 1 lists the diffusion depths at 1323 K of each metal into the other, taken as the distance between the solubility limit and 1 at% (Fig. 3a), i.e., between 25 at% Ni and 1 at% Ni for nickel into rhenium, and between 10 at% Re and 1 at% Re for rhenium into nickel. Assuming a parabolic law common to many diffusion-controlled processes, the diffusion depth can be fitted with reasonable success to the square root of annealing time (Fig. 4), with the diffusion depth at time  $t=0$  within the experimental error of  $\pm 2 \mu\text{m}$ .

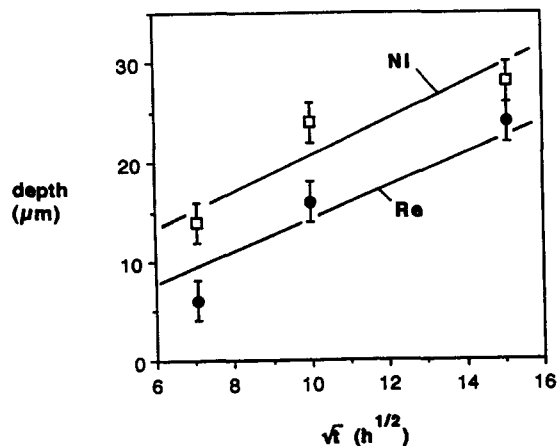


FIG. 4 - Plots of the diffusion depth of nickel into rhenium (marked Ni) and rhenium into nickel (marked Re) as a function of the square root of the annealing time at 1323 K.

**TABLE 2** - Measured Chemical Diffusion Coefficients  $D$  as a Function of Temperature  $T$  and Composition after a 100 h Anneal, and Calculated Activation Energy  $Q$  and Frequency Factor  $A$ .

	T (K)	10 at% Ni	20 at% Ni	95 at% Ni
$D$ (m <sup>2</sup> /s)	1263	8.5 10 <sup>-17</sup>	2.4 10 <sup>-16</sup>	1.3 10 <sup>-16</sup>
$D$ (m <sup>2</sup> /s)	1323	3.1 10 <sup>-16</sup>	1.8 10 <sup>-15</sup>	1.6 10 <sup>-16</sup>
$D$ (m <sup>2</sup> /s)	1383	4.6 10 <sup>-16</sup>	1.2 10 <sup>-15</sup>	6.7 10 <sup>-16</sup>
$Q$ (kJ/mol)		206	199	196
$A$ (m <sup>2</sup> /s)		3.2 10 <sup>-8</sup>	6.0 10 <sup>-8</sup>	1.4 10 <sup>-8</sup>

Matano-Boltzmann analysis techniques (15) were used on smoothed concentration profiles to determine the Matano-Boltzmann interface and chemical diffusion coefficient for various compositions of Samples 2, 4, and 6 (Table 2). Assuming that the chemical diffusion coefficient  $D$  has an Arrhenius form:

$$D = A \exp(-Q/RT) \quad (1)$$

where  $A$  is the frequency factor,  $Q$  the activation energy,  $R$  the gas constant, and  $T$  the temperature, the activation energy and frequency factor were calculated for the above samples by linear regression in a  $\log D$  vs.  $1/T$  plot. Using the parameters  $A$  and  $Q$  given in Table 2, all calculated chemical diffusion coefficients are within a factor of 2 of the measured values, except for Sample 4 ( $T=1323$  K) at 20 at% Ni which exhibits an observed value higher by a factor of 2.4 than the calculated value.

As expected from the shape of the concentration profiles in the rhenium phase (Figs. 3a and 3b), the calculated chemical diffusion coefficients are lower at a concentration of 10 at% Ni than at a concentration of 20 at% Ni at all temperatures. Furthermore, as expected from the similar diffusion depth of each metal into the other (Fig. 4) and the lack of Kirkendall pores (Fig. 2b), the frequency factor and activation energy for the diffusion of nickel into rhenium are of the same order of magnitude as those for the diffusion of rhenium into nickel.

The measured activation energy for the diffusion of nickel into rhenium ( $Q=199-206$  kJ/mol, Table 2) is much lower than that for self-diffusion in rhenium ( $Q=511$  kJ/mol for  $T=1520-1560$  K) (16). It is however close to the value of  $Q=217$  kJ/mol reported by Montelbano *et al.* (5) for the activation energy of the propagation of the nickel-induced recrystallization front in tungsten between 1373 K and 1573 K. This latter activation energy, which is also much lower than the activation energy for self-diffusion in tungsten ( $Q=587$  kJ/mol for  $T=2073-2676$  K), is in qualitative agreement with observations by Hoffmann *et al.* (6), who established that the low-temperature diffusion path for nickel is at tungsten grain-boundaries. We thus propose that the low activation energy values observed in our investigation, similar to that found in the Ni-W system by Montelbano *et al.* (5), may also be explained by diffusion at grain boundaries (or pipe diffusion at dislocations), which typically show activation energy values lower than for bulk diffusion (16). This would also explain why the diffusion depth of nickel into rhenium is not significantly smaller than that of nickel into tungsten, despite the fact that the f.c.c. closed-packed structure of rhenium is expected to exhibit slower nickel bulk diffusion rates than the more open b.c.c. structure of tungsten. Further work is necessary to test this hypothesis, for instance by direct measurements of nickel concentration at rhenium grain boundaries, or by experiments on bicrystals.

The activation energy for self-diffusion of nickel ( $Q=285$  kJ/mol for  $T=1253-1670$  K (16)) is also significantly higher than the measured activation energy for the diffusion of rhenium into nickel ( $Q=196$  kJ/mol, Table 2). However, dislocation self-diffusion and grain boundary self-diffusion in nickel have activation energies of  $Q=104$  kJ/mol ( $T=973-1373$  K) and  $Q=109-127$  kJ/mol ( $T=823-1473$  K) respectively (16). The intermediate value of  $Q=196$  kJ/mol found in the present study may indicate that diffusion of rhenium into nickel results from the combination of bulk and non-bulk paths. The experimental scatter of the three data points used does not however permit to state with certainty that this is the case. Finally, we note that the values of  $D$  for the diffusion of tungsten into nickel (16) and rhenium into nickel (Table 2) are very close in the temperature interval measured. This is not unexpected, since the Goldschmidt radii of tungsten (0.141 nm) and rhenium (0.138 nm) are similar and much larger than that of nickel (0.125 nm) (10).

### Conclusions

Nickel-rhenium diffusion couples were vacuum-annealed at temperatures between 1263 K and 1383 K for times between 50 h and 228 h. The solubility limit of nickel into rhenium is found to be about 25 at% Ni, significantly higher than calculated values (13, 14), but lower than some earlier reports reviewed in Ref. (13). This large solubility and the large measured diffusion depth of nickel into rhenium show that rhenium cannot be used effectively as a diffusion barrier for tungsten fibers in nickel-based metal matrix composites.

Diffusion profiles of nickel into rhenium indicate that the chemical diffusion coefficient is concentration-dependent. The activation energy for the interdiffusion of nickel into rhenium is significantly lower than the self-diffusion coefficients. A possible explanation for this observation is that nickel diffuses into rhenium along grain boundaries, as also observed for the diffusion of nickel into tungsten.

Acknowledgments - This research was supported by Johnson Matthey through an Aesar/Alfa Research Grant, by MIT through an Undergraduate Research Opportunity grant to C.M.N., by the Swiss National Foundation through a postdoctoral grant to D.M., and by AMAX through an endowed chair at MIT for D.C.D. The help of Mr. R.R. Perilli for nickel evaporation is gratefully acknowledged.

### References

1. D. W. Petrasek and R. A. Signorelli: in *International Encyclopedia of Ceramics*, S.M. Lee Ed., VCH, New York, 1990, pp. 332-359.
2. R. Warren: in *9th Risø International Symposium on Metallurgy and Materials Science*, S.I. Andersen, H. Lilholt, and O.B. Pedersen Ed., 1988, pp. 233-255.
3. T. Caulfield and J. K. Tien, *Metall. Trans.* 20A, 255-266 (1987).
4. J. K. Tien, T. Caulfield, and Y. P. Wu, *Metall. Trans.* 20A, 267-272 (1987).
5. T. Montelbano, J. Brett, L. Castleman, and L. Seigle, *Trans. AIME* 242, 1973-1979 (1968).
6. J. Hoffmann, S. Hofmann, and L. Tillmann, *Z. Metallk.* 65, 721-726 (1974).
7. D. C. Dunand and B. Derby: in *Fundamentals of Metal Matrix Composite*, S. Suresh, A. Mortensen, and A. Needleman Ed., Butterworths, London, 1993, pp. 191-214.
8. B. D. Bryskin and F. C. Danek, *JOM* 43 (7), 24-26 (1991).
9. A. J. Sherman, R. H. Tuffias, and R. B. Kaplan, *JOM* 43 (7), 20-23 (1991).
10. E.A. Brandes, and G.B. Brook Ed., *Smithells Metals Reference Book*, 7<sup>th</sup> Ed., Butterworth-Heinemann, Oxford, UK, 1992, pp. 14.1-14.6.
11. E. M. Savitskii and M. A. Tylkina: in *Rhenium*, B.W. Gonser Ed., Elsevier, Amsterdam, 1960, pp. 57-66.
12. J. Crank, *The Mathematics of Diffusion*, Oxford University Press, Oxford, 1989, pp. 104-136.
13. A. Nash and P. Nash, *Bull. Alloy Phase Diag.* 6, 348-350 (1985).
14. H. Okamoto, *J. Phase Equil.* 13, 335 (1992).
15. P. G. Shewmon, *Diffusion in Solids*, Williams Book, Jenks OK, 1983, pp. 29-32.
16. H. Mehrer Ed., *Diffusion in Metals and Alloys (Landolt-Börnstein)*, vol. 26, Springer, Berlin, 1990.